Accepted Article

Viologen Derivatives Extended with Aromatic Rings Acting as Negative Electrode Materials for Use in Rechargeable Molecular Ion Batteries

Minami Kato,* Hikaru Sano, Tetsu Kiyobayashi, and Masaru Yao*[a]

[a]   M. Kato, H. Sano, T. Kiyobayashi, M. Yao
        Research Institute of Electrochemical Energy, Department of Energy and Environment, National Institute of Advanced Industrial
        Science and Technology (AIST)
        1-8-31 Midorigaoka, Ikeda, Osaka 563-8577, Japan
        E-mail: katou.minami@aist.go.jp
                m.yao@aist.go.jp

        Supporting Information and the ORCID identification number(s) for the author(s) of this article can be found under:
        https://doi.org/XXX.

Abstract: Many types of batteries have been proposed as next-generation energy storage systems. One candidate is a rocking-chair-type "molecular ion battery" in which a molecular ion, instead of Li^+, works as a charge carrier. We previously reported a viologen-type derivative as a negative electrode material that releases and receives PF_6^- anions during the charge–discharge process; however, its redox potential was not satisfactorily low. Further, the two potential plateaus of this material (difference = 0.5 V) should be reduced. In this study, PF_6^- salts of viologen (bipyridinium) derivatives extended by aromatic rings were synthesized to obtain a negative electrode material with a lower redox potential and small potential change during the charge and discharge processes. Some of the synthesized viologen derivatives were fluorescent even in the solid-state electrodes. In the half-cell configuration, the prepared negative electrode materials showed average voltages of approximately 2 V (vs. Li), which is lower than conventional viologen derivatives.

Introduction

To meet the increasing electric power demand for operating various electronic devices, including electric vehicles, sustainable, high performance, and environmentally safe batteries are required.[1] One strategy to meet this demand is to improve the widely used rechargeable lithium batteries. However, the use of minor-metal-based positive electrode materials in this battery system cause problems related to environmental burden and cost. In addition, lithium ions as the charge carrier have the potential risk of forming dendrites, which can cause a short circuit in the battery and thermal runaway, which is an unacceptable and dire situation.

As a strategy to solve the problems described above, Yao *et al.* proposed a rocking-chair-type rechargeable battery system that uses neither alkaline metal nor alkaline earth metal elements. Instead, it uses molecular ions as charge carriers; the battery is called a "molecular ion battery,"[2] which overcomes the risk of dendrite formation. In addition, high energy density and low environmental burden are expected for this system when appropriate positive and negative electrode materials are developed. In the first example of this type of battery suggested by Yao *et al.*, the PF_6^- anion functions as a charge carrier, i.e., it is transported between the positive electrode using poly(*N*-vinylcarbazole) (PVK) and the negative electrode using a viologen (bipyridinium) type polymer: poly(1,1'-pentyl-4,4'-bipyridinium dihexafluorophosphate) (PBPy). Here, PBPy undergoes a two-electron transfer redox reaction in two potential plateau regions[2] at −0.7 V and −1.2 V vs. Ag+/Ag. This translates into 2.6 V and 2.1 V vs. Li+/Li, which reflects the redox reaction of the viologen skeleton[3,4] as shown in Figure 1a. At higher potentials, the pristine dicationic viologen structure receives one-electron to form a monocationic radical accompanying

the one counter-anion release. When the potential lowers, the monocationic radical accepts the additional electron to become a neutral quinoid compound. The potential of the positive electrode PVK is around 0.8 V vs. Ag$^+$/Ag (~4.1 V vs. Li$^+$/Li). As a result, the working voltage of the model cell is less than 2 V, which reflects the small potential difference between PVK and PBPy. The potential of PVK may be considered satisfactorily high compared to other reported positive electrode materials; however, there is room for lowering the potential of the negative electrode. To increase the battery working voltage of an anion-based molecular ion battery, the redox potential of the negative electrode material should be lower. In addition, it is preferable for the electrode material to have a small potential charge during the charge/discharge processes because it leads to stable battery voltage during operation.

To satisfy these requirements, we considered inserting aromatic rings into the viologen skeleton as this can effectively induce π-conjugation and charge-separation effects. With this insertion, the energy level of the redox-relating orbitals of the extended viologen skeletons can be expected to become higher than that of normal methyl viologen, which will contribute to lowering average voltage. Further, charge separation in the molecule would reduce the interaction between the two pyridinium moieties, which should then make the potential change during the two-electron transfer reaction smaller. In this study, to verify this hypothesis, we synthesized PF$_6^-$ salts of extended viologen derivatives in which two pyridinium rings of the viologen were separated by the phenylene, thiophene, 3,4-ethylenedioxythiophene, and pyridine rings (**1**–**4** in Figure 1b). The compounds were evaluated as the negative electrode material for use in molecular ion batteries. As a result, these extended viologen derivatives were charged and discharged with a smaller change in the plateau potential at a lower redox potential (~2 V vs. Li$^+$/Li) than the PBPy (2.1 and 2.6 V vs. Li$^+$/Li). Therefore, the working voltage of the extended viologen derivatives can exceed 2 V with the PVK cathode. In this study, a molecular anion (PF$_6^-$) is used as a charge carrier. The presented extended viologen derivatives are potential candidates for negative electrode materials that exceed PBPy in energy density. The capacity of the negative electrode in the previous paper[2] was adjusted to be more than twice that of the positive electrode to utilize the lower potential region of the negative electrode. We incidentally discovered the fluorescent phenomenon of these compounds, for which the properties depend on the cross-linking site of the molecule, even when used at the solid state. In the latter part of this paper, we describe a DFT-based quantum chemistry calculation

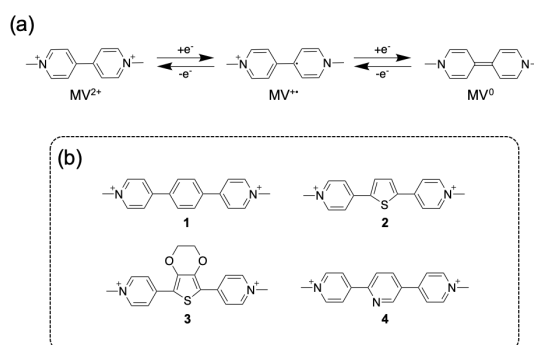that predicts certain model compounds with a lower potential.

Figure 1. (a) Redox scheme of methyl viologen (MV) and (b) extended viologen derivatives (compounds **1**–**4**).

Results and Discussion

Synthesis

A series of viologen derivatives bridged by aromatic rings were synthesized—as shown in Figure 2—according to the method reported by Ryan et al.[5] and Yao et al.[2]. First, the pyridine skeleton and corresponding aromatic ring were connected using the Pd-catalyzed Suzuki-coupling condition. The prepared triad precursors were then quaternized by iodomethane to yield the desired extended viologen skeletons. The final derivatives were obtained via ion exchange from I$^-$ to PF$_6^-$.
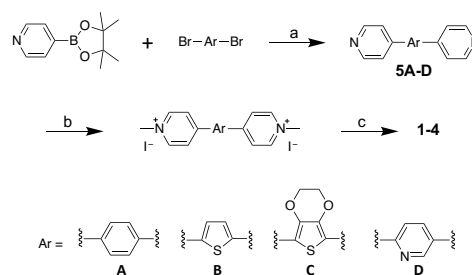
Scheme 1. Synthesis route of compounds **1**–**4**. Regents and conditions: a) Pd(PPh$_3$)$_4$, K$_2$CO$_3$, 1,4-dioxane, toluene, 80 °C; b) CH$_3$I, CH$_3$CN; c) NH$_4$PF$_6$, H$_2$O, r.t..

Photochemical properties

Fluorescent properties were previously reported for compounds **1** and **2** in CH₃CN at room temperature.[6] Before the battery test, the effect of the chemical structure on the fluorescence properties was investigated by comparing **1**–**4**. The fluorescence of small viologen derivatives, such as MV, is difficult to observe by the naked eye because it is in the ultraviolet region at around 350 nm.[7] As reported,[6] **1** and **2** emit fluorescence in CH₃CN (Figure S1). The excitation maximum wavelengths of **1** and **2** are 322 and 360 (sh 383) nm, respectively, and the fluorescence maximum wavelengths are 377 and 416 (shoulder, sh, 427) nm, respectively; these results are similar to those reported in the literature[6]. The excitation maximum wavelength of **3** is 368 nm and the maximum wavelength of the fluorescence is 479 nm. The fluorescence of **4** is very weak, probably because of the proximity in the energy levels of the π-π* and n-π* transitions in the pyridine ring[8] and the hydrogen bond formed between the nitrogen atom and the solvent, respectively. Compounds **1**, **2**, and **3** emit fluorescence in ethylene glycol (EG), a more polar solvent than CH₃CN, at room temperature (Figures 2a-c). Photophysical data are summarized in Table 1. As in CH₃CN, **4** was not fluorescent in EG. Among the compounds, **2** has the highest fluorescence intensity, which reflects its highest fluorescence quantum yield (Φ_f).

Fluorescence and excitation spectra in the solid state were also examined. Compound **1** emitted slightly bluish white light and **2** emitted yellowish green light. Their maximum fluorescence at the longer wavelength side in the spectra (Figures 2d and e) and quantum yields were both less than 10%. In addition, precursors **5A–D** were fluorescence active; **5A** and **5D** emitted blue light and **5B** and **5C** emitted yellow light in the solid state when irradiated with the 365-nm UV light. The excitation and emission spectra of precursors **5A–D** in CH₃CN are shown in Figure S2. If we are to utilize the fluorescence—to suppress concentration quenching—it would be necessary to take measures such as introducing bulky substituents and increasing the rigidity of the structure.[9–15]

The fluorescence properties of compounds **1–4** in the solid electrode state, i.e., in the electrode, were examined and the results are shown in Figure 3. These electrodes were fabricated using a carbon-based conductive additive (acetylene black: AB). The electrodes containing **2** and **3** are fluorescent. Under a black light, the electrodes **2** and **3** emitted yellowish green light (Figure 3e). Although electrodes using **1** and **4** lack strong emission, they emitted a bluish light when AB was replaced by a polymer-based conductive composite (PEDOT/PSS/D-sorbitol) (Figure S3). The carbon-based additive AB is believed to absorb the bluish light and quench the fluorescence.[16,17] These fluorescence characteristics of the electrodes can be used for indicating the state of charge (SOC) of the batteries when a transparent window is provided.
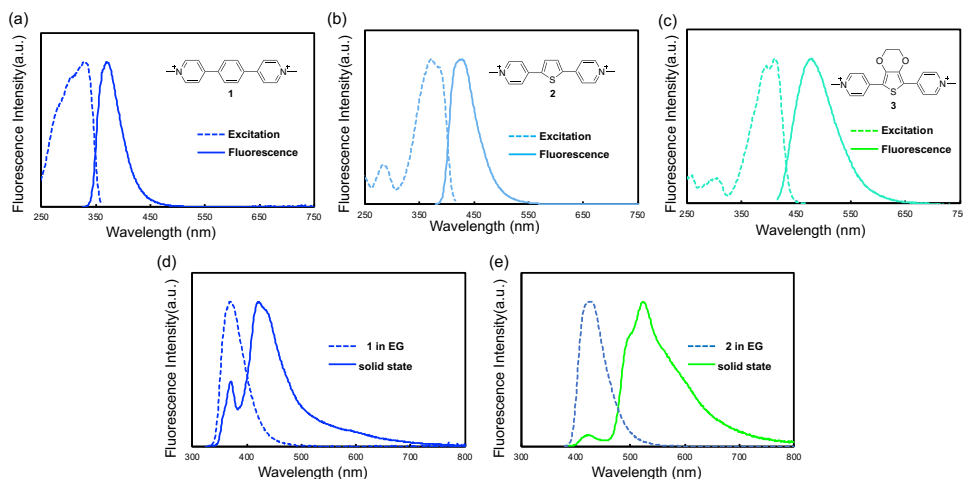

Figure 2. Excitation and fluorescence spectra of (a) **1**, (b) **2**, and (c) **3** in EG and the fluorescence spectra in the solid state for (d) **1** and (e) **2**.
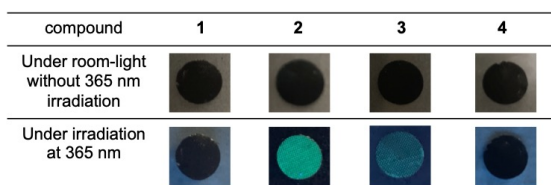
Figure 3. Pictures of the electrodes of compounds **1**–**4** using a carbon-based conductive additive under room light (top) and a black light (bottom).

Table 1. Photophysical properties of conjugation-extended viologens, **1**, **2**, and **3** in EG. (sh: Shoulder)

Compound	Excitation (λ_{max}/nm)	Fluorescence (λ_{max}/nm)	$\Delta\lambda$ (nm)	Quantum yield (Φ_f)
1	331, sh309, sh284	370	39	0.61
2	375, sh390	426	51	0.83
3	397, 413	479	82	0.06

Electrochemical performance

The electrochemical performances of **1**–**4** were measured using a coin-type Li-half-cell. The charge–discharge curves and cycle characteristics for each cell are shown in Figures 4a-d and Figure S4. The theoretical capacities—assuming a two-electron transfer reaction per each molecule—are 97, 96, 81, and 97 mAh g^{-1} for **1**, **2**, **3**, and **4**, respectively. The initial anodic capacity was 70 (**1**), 67 (**2**), 54 (**3**), and 65 (**4**) mAh g^{-1}. (The initial cathodic capacity of these compounds exceeds each of their theoretical value, to which, we suspect, a shuttle effect of soluble species or an irreversible reaction at the interface might be related.) The average voltages during the anodic process of the lithium half cells using **1**, **2**, **3**, and **4** were 1.98, 2.12, 2.07, and 2.10 V, respectively, vs. Li C.E. These values are lower than those previously reported for viologen polymers connected by a short saturated chain (2.1 and 2.6 V vs. Li$^+$/Li).[2] As for the conventional viologen skeleton, we examined 1,1'-di-*n*-octyl-4,4'-bipyridinium to confirm its two plateau regions around 2.1 and 2.5 V vs. Li C.E. during the anodic process (Figure S5). As for the voltage differences between the plateau regions during the anodic process, the observed values were 0.15, 0.32, 0.34, and 0.26 V for **1**, **2**, **3**, and **4**, respectively. The ring expansion narrows the voltage gap between the two plateau regions from 0.5 V for the conventional viologen to about 0.2–0.3 V for **1**–**4.**

The experimental results validate the hypothesis that aromatic spacers can lower the potential of the viologen skeleton and narrow down potential gaps. The degree of this function was different depending on the kind of spacers. Takahashi *et al.* [5] and Ryan *et al.* [6] independently examined the redox behaviors of the benzene-inserted one, **1**, and thiophene-derivative, **2**, in the solution state. According to their results, the benzene derivatives show a lower potential than the thiophene-one, which agrees with our experimental results; however, our samples are in the solid state. Compared to the six-membered benzene ring, the five-membered thiophene ring is classified as a π-electron-rich system, which affects the electronic state of the redox centers. While the redox behaviors of **3** and **4** have not been so far reported, the electron donating ethylenedioxy substituent and the electron deficient pyridine ring can also affect the redox behaviours. However, they showed similar average voltages and voltage gaps to **1** and **2,** and no significant difference is observed. In addition to the factors described above, the dihedral angle between the aromatic spacers and the peripheral pyridinium ring reflecting the steric effect of the spacers and crystal structure differences are considered to slightly affect the redox behaviors. The sizes of the inserted spacers have a major effect on reducing the interaction between the two pyridinium centres in our case.

As for the cycle performance, all prepared cells deteriorated upon cycling; the anodic capacities dropped to 38 and 47 mAh g^{-1} after 10 cycles for **1** and **4**, respectively, while those of **2** and **3** dropped to about 10 mAh g^{-1} (Figure S4). After ten charge–discharge cycles, each cell was disassembled at the anion-released state. The separators were colored in the **2**/Li, **3**/Li, and **4**/Li cells, but not in the **1**/Li cell. The disassembled cell components emitted fluorescence under black light, including those in the **1**/Li cell (Figure S6); this suggests that the dissolution of the active materials into the electrolyte solutions during cycling resulted in a short cycle life for these cells. The synthesized extended viologen derivatives do not dissolve in the electrolyte solution of EC/DEC easily; however, the solubility of their reduced species is considered to become higher than that of the pristine ones. To improve the cycle life, the suppression of the dissolution of the reduced states is inevitable. Therefore, the polymerization and/or oligomerization of redox centers would be effective.[18–22] In fact, some

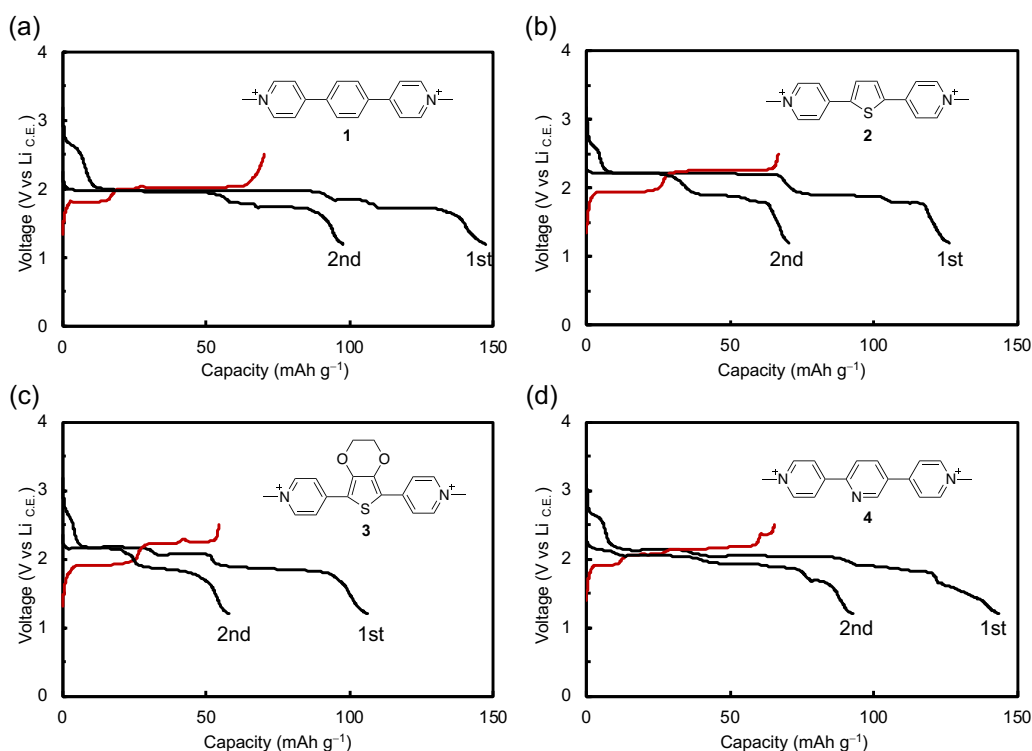viologen polymers such as the above-mentioned PBPy, have a longer cycle life than the monomers.

Figure 4. The 1st cathodic–anodic curves and the following 2nd cathodic curve for electrodes **1**−**4** at a current density of 20 mAh g^{-1} (~0.2 C) at 30 °C. 1.0 mol L^{-1} LiPF$_6$ in EC/DEC (= 1/5 v/v) was used as the electrolyte solution.

Quantum chemistry calculation

In this section, a model compound **5**, in which the anthracene skeleton was inserted between the two pyridyl groups, was calculated based on the DFT method. The one-electron-reduced cation radicals were calculated as they represent the average state of the two-electron transfer during the charge–discharge process. Figure 5 shows the optimized structure along with the energy level of the singly occupied molecular orbitals. Compounds **1**−**4** are virtually planar, and they reflect the double-bonding nature of the bridging bond in radical species. Numerical data are summarized in Table 2. As can be seen in the figure and the table, singly occupied molecular orbitals are split into two different energy levels—SOMO-α and SOMO-β—of which the average energy (E_{SOMO}) for the radicals of **1**−**4** is about 0.6–0.8 eV higher than that of the MV radical. This result points to the lower redox potential of **1**−**4** compared to MV, which likely stems from the larger

π-conjugation system of the former and corroborates the experimental result well. The energy gap, $\Delta E_{SOMO} = |E_{SOMO-\alpha} - E_{SOMO-\beta}|$, should positively correlate with the voltage difference between the first and second plateaus, $\Delta E_{plateau} = |E_{1st\ plateau} - E_{2nd\ plateau}|$. The present calculated result, ΔE_{SOMO} for the MV radical (0.37 eV), is greater than those for the radical states of **1**−**4** (0.25–0.27 eV). The calculated potential difference values did not exactly match the actually observed for **1**−**4** probably because of the lack of a solid-state effect in this calculation. However, this simple calculation well explains the experimental observation that the compounds synthesized in the present study have narrower $\Delta E_{plateau}$ than MV. Furthermore, our calculation predicts further lowering in the potential and narrowing in $\Delta E_{plateau}$ for **5**, beyond the present viologen derivatives **1**−**4**.
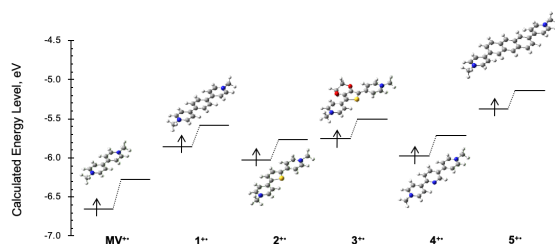
Figure 5. Optimized structures of one-electron-reduced radical cation states of a series of viologen derivatives and the energy levels of their singly occupied molecular orbitals (SOMOs), obtained by the density function theory (DFT) method (UBLYP/6-31G*).

Table 2. Energy levels of the SOMOs of one-electron-reduced cation radical species for **1**−**5** calculated using the DFT method (UBLYP/6-31G*).

Compound	Calculated E_{SOMO} /eV			
	SOMO-α	SOMO-β	Average	Δ
MV$^{+\cdot}$	−6.65	−6.28	−6.47	0.37
1$^{+\cdot}$	−5.86	−5.59	−5.72	0.27
2$^{+\cdot}$	−6.02	−5.76	−5.89	0.26
3$^{+\cdot}$	−5.75	−5.50	−5.63	0.25
4$^{+\cdot}$	−5.97	−5.72	−5.85	0.26
5$^{+\cdot}$	−5.37	−5.14	−5.25	0.23

Conclusion

We synthesized and investigated viologen derivatives, in which two pyridinium skeletons were bridged by several types of aromatic rings, to develop a negative electrode material for use in a rocking-chair-type "molecular ion battery."[2] The redox potential of these derivatives is approximately 2 V vs. Li C.E., which is lower than that of other viologen derivatives previously reported (~2.3 V vs. Li C.E.). A maximum anodic capacity of 70 mAh g^{-1} was observed for a benzene ring inserted derivative, **1**, which corresponds to 72% of the theoretical capacity. In addition, some of the synthesized derivatives emitted fluorescence, even in the solid state, which can be applied as a SOC indicator. As illustrated in the study, the characteristics of organic compounds, such as the redox potential, color, and fluorescence, can be controlled by adjusting the skeleton structure. The synthesized extended viologen derivatives need to be improved in terms of cycle

stability and energy density. As stated in the section on electrochemical performance, the next step in this study is to improve the cycle characteristics by polymerizing derivatives such as **1**, which work at a low voltage that suppresses the dissolution of low molecular weight compounds. Further, to increase the total energy density of a full cell, another design to realize the higher capacity anode material would be simultaneously necessary.

In addition to the battery materials described in this study, extended viologens can be used in various fields, such as organic electroluminescence, organic solid-state lasers, and organic fluorescent molecular sensors.

Experimental Section

Materials

The reagents 1,4-dibromobenzene (>99.0%), 4-(4,4,5,5-tetramethyl-1,3,2-dioxaborolan-2-yl)pyridine (>98.0%), 2,5-dibromothiophene (>95.0%), 2,5-dibromo-3,4-ethylenedioxythiophene (>98.0%), and 2,5-dibromopyridine (>99.0%), were purchased from Tokyo Chemical Industry (Japan). The electrolyte solution was prepared by dissolving 1.0 mol L^{-1} of lithium hexafluorophosphate (PF$_6$) (LiPF$_6$, Kishida Chemical, Japan) in an EC - diethyl carbonate (DEC) co-solvent (1:5 v/v), which was prepared by mixing EC solvent (1:1 v/v, Kishida Chemical, Japan) and DEC solvent (Kishida Chemical, Japan).

Electrochemistry

Electrodes: The composite electrodes for the battery test were prepared by mixing the extended viologen derivatives as the active material, acetylene black as the conductive additive, and polytetrafluoroethylene as the binder in the weight ratio of 4:5:1. The composite was pressed on an Al mesh and dried at 120 °C under vacuum for 1 h. The electrode using a PEDOT/PSS/sorbitol conductive composite material was prepared following the method in our previous study.[23]

Coin-type cells: The prepared electrode, acting as a working electrode, separator (glass filter), electrolyte (1 mol L^{-1} LiPF$_6$ in EC/DEC (= 1/5 v/v)) and lithium-metal, as a counter electrode, were placed in an IEC R2032 coin-type cell in a dry chamber (D.P. < −70 ºC).

Battery test: The half cells were initially galvanostatically discharged, during which the anion is released and subsequently charged at the current density of 20 mA g^{-1}, corresponding to ca. 0.2 C based on the theoretical capacity of the present compounds, with the cut-off voltage window of 1.2–

3.5 V vs. Li C.E. The discharging in the half-cell setup corresponds to charging in the full-cell setup when the working electrode is considered a negative electrode. A battery evaluation system (BLS series, Keisokuki Center, Japan) was used at a temperature maintained at 30 °C.

Photochemical properties: Photoluminescence (PL) and UV-vis spectra were recorded with a multichannel PL analyzer (Hamamatsu, PMA-12) and a UV-vis spectrometer (JASCO, V-670). The PL quantum yields were measured by attaching an integrating sphere to the PL spectrometer. The PL lifetimes were recorded with a time-correlated single-photon counting setup (Hamamatsu, Quantaurus-Tau).

Synthesis of extended viologen derivatives

Compounds **1**–**4** were synthesized according to the methods in the references.[2][5] The prepared materials were characterized by NMR spectroscopy (JHM-ECS series, JEOL, v(^{1}H) = 400 MHz) and a mass spectrometer (ACQUITY SQD, Waters) equipped with an atmospheric solid analysis probe.

Phenylene-inserted extended viologen PF$_6$ salt (1): The reagents 1,4-dibromobenzene (474 mg, 2.00 mmol), 4-(4,4,5,5-tetramethyl-1,3,2-dioxaborolan-2-yl) pyridine (1.44 g, 7.00 mmol), K$_2$CO$_3$ (2.16 g, 15.6 mmol) and Pd(PPh$_3$)$_4$ (235 mg, 0.20 mmol) were added to the 1:1 mixture dry-solvent, toluene (6 ml) and 1,4-dioxane (6 ml) and distilled H$_2$O (3 ml). The solution was stirred at 80–90 °C under an Ar atmosphere for 72 h. The reaction mixture was concentrated under vacuum, dissolved in CH$_2$Cl$_2$, then extracted twice and washed three times with H$_2$O. The obtained organic layer was added with Na$_2$SO$_4$ and filtered with a cotton plug, and then, the solution was concentrated under vacuum. The obtained solid was recrystallized with CH$_2$Cl$_2$/hexane to obtain a white solid powder of the precursor (dipyridiyl benzene: **5A**) (417 mg, 89.7%). ^{1}H NMR (400 MHz, DMSO-d_6): δ = 8.64(d, J = 4.4 Hz, 4H), 7.94 (s, 4H), 7.76 (d, J = 4 Hz, 4H); MS (m/z) 232 (M$^-$). The dipyridyl precursor **5A** (204 mg, 0.86 mmol) was added to MeI (0.5 ml, 8.6 mmol) and stirred in 40 ml CH$_3$CN at 90 °C overnight. The reaction solution was added with CH$_2$Cl$_2$ and then filtered *in vacuo* to obtain a reaction mixture. The obtained solid was dissolved in 40 ml H$_2$O and then 2.5 ml of saturated NH$_4$PF$_6$ aqueous solution was added and stirred at room temperature for 3 h. The precipitate was filtered, washed with H$_2$O and CH$_3$OH, and dried *in vacuo* to obtain pure **1** as a white solid (384 mg, 82.4%). ^{1}H NMR (400 MHz, DMSO-d_6): δ = 9.05 (d, J = 6 Hz, 4H), 8.60 (d, J = 6 Hz, 4H), 8.30 (s, 4H), 4.32 (s, 6H); MS (m/z) 262 [M−2PF$_6$]$^-$.

Thiophene-inserted extended viologen PF$_6$ salt (2) : The reagents 2,5-dibromo-3,4-thiophene (499 mg, 2.00 mmol), 4-(4,4,5,5-tetramethyl-1,3,2-dioxaborolan-2-yl) pyridine (1.45 g, 5.2 mmol), K$_2$CO$_3$ (2.26 g, 16 mmol), and Pd (PPh$_3$)$_4$ (233 mg, 0.2 mmol) were added to H$_2$O (3 ml) and the 1:1 mixture dry-solvent, toluene (6 ml), and 1,4-dioxane (6 ml). The solution was stirred at 80 °C under Ar atmosphere for 72 h. The reaction mixture was concentrated under vacuum, dissolved in CH$_2$Cl$_2$, then extracted twice and washed twice with H$_2$O. The obtained organic layer was added with Na$_2$SO$_4$ and filtered with a cotton

plug; then, the solution was concentrated under vacuum. The obtained solid was recrystallized with CH$_2$Cl$_2$/hexane to obtain a yellow solid of dipyridyl thiophene precursor (**5B**) (371 mg, 63.5%). ^{1}H NMR (400 MHz, DMSO-d_6): δ = 8.58 (dd, J = 4.4, 1.2 Hz, 4H), 7.89 (s, 2H), 7.68 (dd, J = 4.4, 1.2 Hz, 4H); MS (m/z) 238 (M$^-$). The precursor **5B** (102 mg, 0.36 mmol) was added to MeI (0.25 ml, 4.0 mmol) and stirred in 30 ml CH$_3$CN at 90 °C overnight. The reaction solution was added with CH$_2$Cl$_2$, and then filtered *in vacuo*, to obtain a reaction mixture. The obtained solid was dissolved in 30 ml H$_2$O and then 1 ml of saturated NH$_4$PF$_6$ aqueous solution was added and stirred at room temperature for 30 min. The precipitate was filtered, washed with H$_2$O and CH$_3$OH, and dried *in vacuo* to obtain pure **2** as a yellow solid. (155 mg, 78%). ^{1}H NMR (400 MHz, DMSO-d_6): δ = 8.96 (d, J = 7.2 Hz, 4H), 8.42 (d, J = 7.2 Hz, 4H), 8.40 (s, 2H), 4.27 (s, 6H); MS (m/z) 268 [M−2PF$_6$]$^-$.

Ethylenedioxythiophene-inserted extended viologen PF$_6$ salt (3): The reagents 2,5-dibromo-3,4-ethylenedioxythiophene (596 mg, 2.00 mmol), 4-(4,4,5,5-tetramethyl-1,3,2-dioxaborolan-2-yl) pyridine (1.08 g, 5.2 mmol), K$_2$CO$_3$ (2.22 g, 16 mmol), and Pd (PPh$_3$)$_4$ (234 mg, 0.2 mmol) were added to H$_2$O (3 ml) and the 1:1 mixture dry-solvent, toluene(6 ml), and 1,4-dioxane (6 ml). The solution was stirred at 85 °C under an Ar atmosphere for 72 h. The reaction mixture was concentrated under vacuum, dissolved in CH$_2$Cl$_2$, then extracted three times and washed twice with H$_2$O. The obtained organic layer was added with Na$_2$SO$_4$ and filtered with a cotton plug, and then, the solution was concentrated under vacuum. Recrystallization with CH$_2$Cl$_2$/hexane yielded a yellow solid of dipyridyl precursor **5C** (510 mg, 86.8%). ^{1}H NMR (400 MHz, DMSO-d_6): δ = 8.57 (dd, J = 4.8, 1.6 Hz, 4H), 7.62 (dd, J = 4.4, 1.2 Hz, 4H), 4.43 (s, 4H); MS (m/z) 296 (M$^-$). **5C** (204.5 mg, 0.67 mmol) was added with MeI (0.45 ml, 6.7 mmol) and stirred in 50 ml CH$_3$CN at 50 °C overnight. The reaction solution was added with CH$_2$Cl$_2$, and then filtered *in vacuo* to obtain a reaction mixture. The obtained solid was dissolved in 40 ml H$_2$O and then a solution of 4.06 g NH$_4$PF$_6$ dissolved in 5 ml H$_2$O was added and stirred at room temperature for 3 h. The precipitate was filtered, washed with H$_2$O and CH$_3$OH, and dried *in vacuo* to yield pure **3** as a yellow solid (352 mg, 82.4%). ^{1}H NMR (400 MHz, DMSO-d_6): δ = 8.87(d, J = 6 Hz, 4H), 8.26 (d, J = 6 Hz, 4H), 4.61 (s, 4H), 4.25 (s, 6H); MS (m/z) 326 [M−2PF$_6$]$^-$.

Pyridine-inserted extended viologen PF$_6$ salt (4): The reagents 2,5-dibromopyridine (476 mg, 2.0 mmol), 4-(4,4,5,5-Tetramethyl-1,3,2-dioxaborolan-2-yl)pyridine(1.0330 g, 5.0 mmol), and K$_2$CO$_3$ (2.22 g, 16 mmol), Pd (PPh$_3$)$_4$ (234 mg, 0.2 mmol) were added to water (3 ml) and the 1:1 mixture dry-solvent, toluene (6 ml), and 1,4-dioxane (6 ml). The solution was stirred at 80 °C under an Ar atmosphere for 72 h. The reaction mixture was concentrated under vacuum, dissolved in CH$_2$Cl$_2$, then extracted three times and washed three times with H$_2$O. The obtained organic layer was added with Na$_2$SO$_4$ and filtered with a cotton plug, and then, the solution was concentrated under vacuum. Subsequent recrystallization yielded a white solid of the dipyridyl precursor, **5D** (323 mg, 68.8%). ^{1}H NMR (400 MHz, DMSO-d_6): δ = 9.17 (s, 1H), 8.71–8.67 (m, 4H), 8.38 (d, J = 8.4 Hz, 1H), 8.26 (d, J = 8.8 Hz, 1H), 8.10 (d, J = 4.8 Hz, 2H), 7.85 (d, J = 4.8 Hz, 2H); MS (m/z) 233

(M⁻). The powder of **5D** (201 mg, 0.86 mmol) was added to MeI (0.5 ml, 8.0 mmol) and stirred in 40 ml CH_3CN at 80 °C overnight. The reaction solution was added with CH_2Cl_2, and then filtered *in vacuo* to obtain a reaction mixture. The obtained solid was dissolved in 40 ml H_2O and then a solution of 4.06 g NH_4PF_6, dissolved in 5 ml H_2O, was added and stirred at room temperature for 3 h. The precipitate was filtered, washed with H_2O and CH_3OH, and dried *in vacuo* to yield pure **4** as a white solid (424 mg, 88.9%). ¹H NMR (400 MHz, DMSO-d_6): δ = 9.45 (s, 1H), 9.18–9.02 (m, 4H), 8.84 (d, J = 5.2 Hz, 2H), 8.77 (d, J = 8.4 Hz, 1H), 8.67 (d, J = 5.2 Hz, 2H), 8.64 (s, 1H), 4.36 (d, J = 8 Hz, 6H); MS (*m/z*) 263 [M−2PF₆]⁻.

Density functional theory (DFT) calculation

The most stable structures of the one-electron reduced cation radical states of **1**–**4** were calculated by the DFT method using the combination of an unrestricted hybrid functional of UBLYP and a basis set of 6-31G(d) using the Gaussian 03 package.[22]

Acknowledgments

Keywords: Energy storage • Organic battery • Molecular ion battery • Fluorescence • Redox chemistry

[1]   J. B. Goodenough, *Energy Environ. Sci.* **2014**, *7*, 14–18.
[2]   M. Yao, H. Sano, H. Ando, T. Kiyobayashi, *Sci. Rep.* **2015**, *5*, 1–8.
[3]   A. Iordache, R. Kannappan, E. Métay, M. C. Duclos, S. Pellet-Rostaing, M. Lemaire, A. Milet, E. Saint-Aman, C. Bucher, *Org. Biomol. Chem.* **2013**, *11*, 4383–4389.
[4]   J. Ding, C. Zheng, L. Wang, C. Lu, B. Zhang, Y. Chen, M. Li, G. Zhai, X. Zhuang, *J. Mater. Chem. A* **2019**, 23337–23360.
[5]   S. T. J. Ryan, R. M. Young, J. J. Henkelis, N. Hafezi, N. A. Vermeulen, A. Hennig, E. J. Dale, Y. Wu, M. D. Krzyaniak, A. Fox, et al., *J. Am. Chem. Soc.* **2015**, *137*, 15299–15307.
[6]   K. Takahashi, T. Nihira, K. Akiyama, Y. Ikegami, E. Fukuyo, *J. Chem. Soc. Chem. Commun.* **1992**, *453*, 620–622.
[7]   J. Peon, X. Tan, J. D. Hoerner, C. Xia, Y. F. Luk, B. Kohler, *J. Phys. Chem. A* **2001**, *105*, 5768–5777.
[8]   E. C. Lim, *J. Phys. Chem.* **1986**, *90*, 6770–6777.
[9]   A. Wakamiya, K. Mori, S. Yamaguchi, *Angew. Chemie - Int. Ed.* **2007**, *46*, 4273–4276.
[10]   A. Iida, S. Yamaguchi, *Chem. Commun.* **2009**, 3002.
[11]   S. Chen, J. Liu, Y. Liu, H. Su, Y. Hong, C. K. W. Jim, R. T. K. Kwok, N. Zhao, W. Qin, J. W. Y. Lam, et al., *Chem. Sci.* **2012**, *3*, 1804–1809.
[12]   Y. Fujiwara, R. Ozawa, D. Onuma, K. Suzuki, K. Yoza, K. Kobayashi, *J. Org. Chem.* **2013**, *78*, 2206–2212.
[13]   A. Sakai, E. Ohta, Y. Yoshimoto, M. Tanaka, Y. Matsui, K. Mizuno, H. Ikeda, *Chem. - A Eur. J.* **2015**, *21*, 18128–18137.
[14]   H. Liu, L. Yao, B. Li, X. Chen, Y. Gao, S. Zhang, W. Li, P. Lu, B. Yang, Y. Ma, *Chem. Commun.* **2016**, *52*, 7356–7359.
[15]   S. Sekiguchi, K. Kondo, Y. Sei, M. Akita, M. Yoshizawa, *Angew. Chemie Int. Ed.* **2016**, *55*, 6906–6910.
[16]   M. C. F. Soares, M. M. Viana, Z. L. Schaefer, V. S. Gangoli, Y. Cheng, V. Caliman, M. S. Wong, G. G. Silva, *Carbon N. Y.* **2014**, *72*, 287–295.
[17]   E. Carata, B. Anna Tenuzzo, F. Arnò, A. Buccolieri, A. Serra, D. Manno, L. Dini, *Int. J. Mol. Cell. Med.* **2012**, *1*, 30–8.
[18]   Y. Inatomi, N. Hojo, T. Yamamoto, S. Watanabe, Y. Misaki, *Chempluschem* **2012**, *77*, 973–976.
[19]   T. Nokami, T. Matsuo, Y. Inatomi, N. Hojo, T. Tsukagoshi, H. Yoshizawa, A. Shimizu, H. Kuramoto, K. Komae, H. Tsuyama, et al., *J. Am. Chem. Soc.* **2012**, *134*, 19694–19700.
[20]   M. Kato, K. Senoo, M. Yao, Y. Misaki, *J. Mater. Chem. A* **2014**, *2*, 6747.
[21]   Z. Zhu, M. Hong, D. Guo, J. Shi, Z. Tao, J. Chen, *J. Am. Chem. Soc.* **2014**, *136*, 16461–16464.
[22]   M. Yao, H. Sano, H. Ando, T. Kiyobayashi, N. Takeichi, *ChemPhysChem* **2019**, *20*, 967–971.
[23]   M. Kato, H. Sano, T. Kiyobayashi, N. Takeichi, M. Yao, *MRS Commun.* **2019**, *9*, 979–984.
[24]   M. J. Frisch, G. W. Trucks, H. B. Schlegel, G. E. Scuseria, M. A. Robb, J. R. Cheeseman, J. A. Montgomery, Jr., T. Vreven, K. N. Kudin, J. C. Burant, J. M. Millam, S. S. Iyengar, J. Tomasi, V. Barone, B. Mennucci, M. Cossi, G. Scalmani, N. Rega, G. A. Petersson, H. Nakatsuji, M. Hada, M. Ehara, K. Toyota, R. Fukuda, J. Hasegawa, M. Ishida, T. Nakajima, Y. Honda, O. Kitao, H. Nakai, M. Klene, X. Li, J. E. Knox, H. P. Hratchian, J. B. Cross, V. Bakken, C. Adamo, J. Jaramillo, R. Gomperts, R. E. Stratmann, O. Yazyev, A. J. Austin, R. Cammi, C. Pomelli, J. W. Ochterski, P. Y. Ayala, K. Morokuma, G. A. Voth, P. Salvador, J. J. Dannenberg, V. G. Zakrzewski, S. Dapprich, A. D. Daniels, M. C. Strain, O. Farkas, D. K. Malick, A. D. Rabuck, K. Raghavachari, J. B. Foresman, J. V. Ortiz, Q. Cui, A. G. Baboul, S. Clifford, J. Cioslowski, B. B. Stefanov, G. Liu, A. Liashenko, P. Piskorz, I. Komaromi, R. L. Martin, D. J. Fox, T. Keith, M. A. Al-Laham, C. Y. Peng, A. Nanayakkara, M. Challacombe, P. M. W. Gill, B. Johnson, W. Chen, M. W. Wong, C. Gonzalez, J. A. Pople, Gaussian 03, Revision E.01, **2004**, Gaussian, Inc., Wallingford, CT.

Entry for the Table of Contents
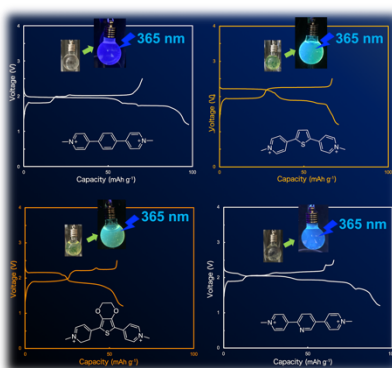
A series of viologen derivatives extended by aromatic rings were synthesized as a negative electrode material to improve the working voltage of anion-based molecular ion batteries wherein PF_6^- works as a charge carrier. These derivatives exhibited lower redox potential than conventional viologen derivatives. Further, the potential difference during the anodic process decreased. Electrodes containing compounds **2** and **3** were fluorescent, which can be applied as SOC indicators.